Life Science Informatics Publications
Research Journal of Life Sciences, Bioinformatics, Pharmaceutical and Chemical Sciences
Journal Home page http://www.rjlbpcs.com/
RJLBPCS
ISSN 2454-6348

Original Research Article **DOI: 10.26479/2019.0502.29**

PRODUCTION OF RECOMBINANT PROTEIN IN THE CHLOROPLAST OF *CHLAMYDOMONAS RENHARDTII*: A SYSTEMS BIOLOGY APPROACH

Oluwafemi Davies[1], Malkhey Verma[2*]

1. Doctoral Training Centre ISBML, The Manchester Centre for Integrative Systems Biology, University of Manchester, Manchester, M1 7DN, UK
2. Department of Biochemistry & Microbial Sciences, Central University of Punjab, Bathinda, Punjab, India.

ABSTRACT: Research into recombinant protein production revealed some attractiveness with expression system based on microalgae and plant, for significant cost-savings and production of stable, active and correctly folded recombinant proteins. In this work, we undertook to study the growth of the microalgae, *C. reinhardtii*, for the chloroplast expression of recombinant *E. coli β*-glucuronidase (gus). We characterized the growth and recombinant gus protein yield in autotrophic, heterotrophic and mixotrophic conditions to understand limitations to growth and the protein yields. The maximum specific growth rate for cultures grown at different conditions: mixotrophic cultures (~0.05 h^{-1}), autotrophic cultures (~0.03 h^{-1}) and heterotrophic cultures (~0.025 h^{-1}). The recombinant gus yields determined on the basis of percentage dry cell weight were: mixotrophic cultures (0.038%), autotrophic cultures (0.032%), heterotrophic cultures (0.026%). No detectable recombinant protein burden on the growth rate was observed for the production of recombinant gus in autotrophic and mixotrophic conditions, but significant reduction observed in the heterotrophic condition (~15%). The understanding of the factors that affected the growth of the cultures was used in designing suitable growth strategies in the heterotrophic condition that reduced the limitations and significantly increased growth ~3 fold. Additionally, flux balance analysis of the genome-scale metabolic re-constructed network of algae was used to provide insights and identify limitations by sub-optimal amino acid steady-state fluxes for gus production. Using the cycle of FBA modelling simulation for gus production, experimental verifications of predictions and FBA corrections, a strategy that significantly increased recombinant gus yield in heterotrophic cells by 2 fold.

KEYWORDS: Recombinant protein, *Chlamydomonas renhardtii,* Chloroplast, Metabolic model, Flux Balance Analysis, Growth conditions.

Corresponding Author: Dr. Malkhey Verma* Ph.D.
Department of Biochemistry & Microbial Sciences, Central University of Punjab, Bathinda, Punjab, India. Email Address: malkhey.verma@cup.edu.in, malkhey@yahoo.com

1.INTRODUCTION

The production of proteins by the recombinant technology of sufficient quantity and good quality is increasingly important to biopharmaceutical, biotechnology industries and to research using recombinant proteins [1-3]. The complexity of proteins means that the process for protein synthesis in living systems is best suited for their production, yet the production of recombinant proteins in a cell or whole organism is fraught with different challenges [1]. Amongst these is a need to produce correctly folded and fully functional complex recombinant proteins in cells without loss of biological activity through protein misfolding or aggregation. Other significant challenges can include high capital and operational costs involved with setting up and running the production platform for recombinant proteins including downstream re-naturation processes to recover protein of sufficient quality [1]. These difficulties make recombinant protein expression on a commercial scale very expensive venture. Nevertheless, the commercial scale manufacturing of recombinant proteins with therapeutic and pharmacological properties to treat different disease conditions is continually drawing the attention and investments by biopharmaceutical and biotech industries [1]. The successes of these investments depend on research drives aimed at the development of expression system that is more robust in terms of producing biologically active therapeutic proteins (in commercial quantities and good qualities) and cost-effective in the capital and operational processes [1]. Different expression platform for large-scale production of recombinant protein exists today. Some of these uses transgenic animals, transgenic plants, transgenic insects, mammalian cell culture, Chinese hamster ovary (CHO) cell, bacterial cell, or yeast cell [1, 2]. Amongst these, transgenic plants provide a more attractive prospect for expressing recombinant proteins because they are photosynthetic, leading to relatively inexpensive growth requirements with light used for their energetic [1, 2]. Therefore, in terms of capital and operational costs for producing recombinant proteins in plants are significantly cheaper [1, 2]. In addition, they may be instructed to produce correctly folded and biologically active recombinant proteins in the chloroplast [4-6] Like the plants, microalgae are photosynthetic and could be transformed to express correctly folded biologically active recombinant proteins in the chloroplast [3, 7-11]. The ability of transgenic plants and microalgae to correctly fold complex mammalian and recombinant proteins in the chloroplast avoids problems such as incorrect protein folding, protein aggregation or prion formation. The expressed recombinant proteins accumulate in the chloroplast, an organelle that provides high biological

containment and prevents loss to the environment [12]. Consequently, the recombinant proteins expressed in plants and microalgae can be free of prions, protein aggregation, and pathogenic contamination, and they are generally regarded as safe [2, 4, 8, 13]. These factors make it attractive to use plant or microalgae for expressing recombinant proteins for bio-therapeutic applications or vaccines that may be administered orally [2, 4, 8]. However, for plants, the spread of pollen to the environment presents regulatory concerns about possibilities for transgene to flow to, and contaminate the environment [14, 15]. With microalgae, this drawback does not exist since microalgae propagate vegetatively by asexual cell divisions [16]. The microalgae that has been best characterized biochemically is *Chlamydomonas reinhardtii* [16] making this organism a versatile model for studying recombinant protein production [3, 7, 8, 10, 11, 17] The expression and accumulation of different types of recombinant proteins including human growth factors, vaccines epitomes [11], antibodies and enzymes in *C. reinhardtii* chloroplast has been demonstrated [3, 9, 10]. Despite these successes, the yields of recombinant proteins expressed in the microalgae chloroplast remain low. Typically, recombinant protein yields from about 0.01 – 0.1% of total soluble proteins in the microalgae have commonly reported [7, 9-11, 17, 18], though protein yields appear to depend on the type of recombinant protein or other factors [17]. These researchers used combinations of molecular biology approaches involving genetic modifications, the design of promoter constructs and combinations, codon optimization, and chloroplast transformations to generate transgenic strains capable of increased recombinant protein yield. However, the low yield for recombinant proteins persists for *C. reinhardtii* chloroplast. Only a few reports of recombinant protein yield ≥3% total soluble proteins exist [11, 17]. There might be other factors that reduce the recombinant protein yield in *C. reinhardtii* chloroplast. The synthesis of a protein such as a recombinant protein that is not required by a cell for its growth, maintenance or unneeded by the cell could affect the growth rate of the cell. The fractional reduction in growth rates that result from the synthesis of such unneeded protein, referred to as protein burden or protein cost has been recognised for some time [19, 20-24]. The protein burden is thought to arise due to diversion of cellular resources to produce 'extra proteins' not required for cell growth [20, 21, 23], or due to a competitive and dilution effect on the expression of endogenous proteins [24]. Since the production of proteins is a major energy demanding operation [25], the expression of 'extra proteins' with no usefulness to a cell may suggest wastage to energy (ATP depletion), metabolic stress on the cell such and may result in a cost [26] Protein cost has been demonstrated in bacteria [19-21, 23, 27] and yeast [28] In addition, protein cost of unneeded protein could determine regulatory strategy employed by a cell to affect the yield of the unneeded protein [21, 29, 30] and the yield allowed without cessation of cell growth [27]. Thus whether the low recombinant protein yield in the microalgae may be due to a protein cost remain unknown because no protein cost evaluation has been reported for microalgae. Whether the low yield was due to metabolic limitations in the system

such as limiting amino acid fluxes for recombinant protein production remain unclear. Living systems are robust and self-sustaining systems capable to adapt and respond to perturbations in their metabolic, genetic or hierarchical organization to maintain their homeostasis and ensure survival [31, 32]. By the cell transformation, a cell may be manipulated to produce a certain recombinant protein. However, the cell may likely to experience the recombinant protein production as a perturbation, and its regulatory responses will then tend to counteract the perturbation. The cell may invoke complex metabolic, genetic and signalling regulations to regulate and elicit control mechanisms that maintain their homeostasis in the presence of such perturbations [31-33]. The likely result is that recombinant protein yield may be lower than yield that i expected and in many cases, erratic and unpredictable because the cell may not always engage in the same homeostatic response [31, 32] The model of recombinant protein production in the current work was the expression of *E. coli β*-glucuronidase (gus) in the chloroplast of *C. reinhardtii.* In our study, systems biology approaches that complement and significantly move forward the recombinant protein research in microalgae is presented. The approach will be used to shine light on the growth and recombinant protein production in *C. reinhardtii,* to identify and understand factors that affect growth and reduce recombinant protein yield. We have used a range of experiments, quantitative data analyses, and flux balance analysis (FBA) to gain insights on strategies to improve growth and recombinant protein yield in *C. reinhardtii.* Flux balance analysis is a widely used constraint-based method to analyse the flow of metabolites through the biochemical network under steady-state conditions [34-39]. Reviews on the application of FBA for studying metabolism and analysing flux distributions in metabolic networks have been described [35, 38]. A variety of computational tools are available for use in FBA to perform *in silico* analysis of networks and these have been reviewed recently [40]. Some of these include Cobra Toolbox [41, 42], SurreyFBA [43], FASIMU [44], OptFlux [45], FBA-SimVis [46], and FAME [47]. Typically, models of metabolic networks for FBA methods contain known metabolites, pathways, reactions, genes and the proteins encoded in the biological system of interest [48-52]. Data for building genome-scale metabolic network reconstruction of biological systems are derived from variety of sources including published literature, databases such as genomics, transcriptomics, proteomics, metabolomics, metabolic pathways, cellular localization, interaction data sources, and the biochemical characterization of the networks in particular [48-52]. Today there are different genome-scale models that are analysed using FBA [48-52]. An example is AlgaGEM [49], a genome-scale metabolic model based on *C. reinhardtii* genomes and metabolisms. AlgaGEM is the most recent and comprehensive genome-scale metabolic network reconstruction of algae metabolism incorporating cellular compartments, the functions of over 800 open reading frames, >1800 metabolites and >1700 metabolic reaction in the microalgae. The model is a useful resource for studying, and making *in silico* predictions of algae metabolism, metabolic processes and phenotypes such as growth rate, photosynthesis, and hydrogen production under autotrophic,

heterotrophic and mixotrophic conditions. The utility of the model means it could be adapted, and indeed applied for our study of recombinant protein production in *C. reinhardtii*. FBA will be used to predict the maximal theoretical yield of recombinant gus in the three growth conditions by applying appropriate constraints on the relevant reactions of the algaGEM model based on the experimental flux values measured on *C. reinhardtii*.

2. MATERIALS AND METHODS

Chlamydomonas reinhardtii strains:

cc373 mt+ strain: is a photosynthetic mutant with the *ac-u-c-2-21* deletion mutation [53, 54] in the chloroplast Bam 10 restriction fragment containing the *atpβ* gene [55]. cc373 mt+ strain is non-photosynthetic and does not grow in light [53] but useful as a recipient for transformation based on the rescue of the defective *atpβ* gene [55] cc373 mt+ strain was obtained from the Chlamydomonas Resource Centre, University of Minnesota, USA.

Bam 10::cc373 mt+ strain: is the photosynthetic-rescued strain obtained by transforming cc373 mt+ chloroplast, with plasmid pB10 (a Bam10-based plasmid) designed to rescue the mutant *atpβ* gene with an intact *atpβ* gene. Photosynthetic-rescue of cc373 mt+ without a foreign gene gave rise to the Bam10::cc373 mt+ (control strain) lacking a foreign gene. Bam10::cc373 mt+ strain was provided by Dr. Anil Day (Faculty of Life Sciences, University of Manchester).

Transgenic strains (Gus12-2 and Gus12-B): are photosynthetic-rescued strains obtained by transformation based on the rescue of the defective *atpβ* gene in cc373mt+ with the plasmid pB10 and *E. coli gusA* gene. In both strains, the expression for *gusA* gene was constitutive using endogenous *atpA* promoter and *rbcL* 3' UTR. The Gus12-2 and Gus12-B strains were provided by Dr. Anil Day (Faculty of Life Sciences, University of Manchester).

Culture media preparation (TAP and minimal):

Tris-Acetate and Phosphate (TAP) and Minimal media used for growth were prepared according to methods of Gorman and Levine [56].

Selection and isolation of photosynthetic transformed strains (Bam10::cc373 mt+, GuS12-2, and Gus12-B): The cultures were propagated under selective pressures by growing in minimal medium and in light at 54 μmol photons m^{-2} s^{-1} to select for the photosynthetic transformed strains as described in [55, 57]. Untransformed cc373 mt+ strains did not grow in light and die out under selective pressures leaving culture enriched with photosynthetic transformed strains. Further sub-culturing and propagation steps under the selective pressures were performed for 5 weeks till cultures become homoplasmic [57].

Detection of gus expression:

Expression of gus was detected by an enzymatic method described in [59, 60]. Gus catalyses the hydrolysis of the β-glucuronides e.g. 5-bromo-4-chloro-3-indoxyl glucuronide (*X-gluc*), through a colourless intermediate, into a blue coloured precipitate product, 5'5'-dibromo-4'4'-dichloroindigo.

Cell counting and optical culture density determination:

Total cell counts of the cultures (number of cells per ml) were measured by the hemocytometer method. Optical density measurements of cultures were performed at 600 nm. Standard calibration curves of optical density at 600 nm against culture density were constructed for autotrophic, heterotrophic and mixotrophic cultures to provide the linear dependence of absorbance at 600 nm on the culture density as described by Harris [16]. The correlation factor (2×10^{-7}) obtained from the slope of the linear calibration plot was used to convert culture absorbance into estimates of culture density during growth according to equation 1:

$$Culture\ density = \left(\frac{Optical\ density\ of\ culture\ at\ 600nm}{0.0000002} \right) \quad (1)$$

Growth conditions and determination of maximum specific growth rates:

Cultures were grown in 50 ml culture medium in shake flask (batch) maintained at a constant 25ºC agitated at 90 rpm, either in autotrophic, heterotrophic or mixotrophic condition. The growth of cultures over time was measured by optical density measurements at 600 nm and plotted as functions of culture density (number of cells per ml) against time (h). The growth rate was described in terms of the specific growth rate (μ) with units of h^{-1}. The natural logarithm of culture density during the exponential growth phase (24 – 96 h) was plotted against time, and the maximum specific growth rate (μ_{max}) was determined as the gradient of the linear slope with units of h^{-1}.

Determination of dry cell weight of cultures:

The dry cell weight of cultures was determined using the cells harvest by centrifugation and drying to constant weight method. The weight of dry polypropylene tube was measured at 20ºC. 50 ml of culture with measured culture density was added to the polypropylene dry tube and centrifuged (2000 rpm for five minutes at 20ºC) to harvest cell pellets from the medium. The clear supernatant was carefully discarded, the cell pellets washed thrice with reverse osmosis water, and the supernatant was carefully discarded. The weight of the wet cell pellets and tube was measured (sample), before drying at 60ºC for 12-14 h in an oven (Leader engineering Ltd) until a constant dry weight was obtained. Samples were weighed repeatedly within a 3 minute time window at 20ºC to determine constant dry weight measurement. The microalgae dry cell weight was calculated in units of gram dry weight per cell.

Culture harvest and protein extraction:

Methods for culture harvest, cell lysis by sonication and protein extraction were adapted from Jefferson, Jefferson et. al., and Rochaix et al., [57, 58, 61]. 10 ml cultures of known densities were collected during the exponential growth phase and centrifuged at 2000 rpm for five minutes at 4ºC. The cell pellets were collected and re-suspended with 3 ml gus extraction buffer pH 7 [58, 59]. The 10 ml supernatant fraction was collected, and filtered through a 0.22 μm sterile filter to remove suspended cells. The 10 ml filtrate (extracellular medium) were concentrated (10X) by ultra-

filtration in the vivaspin 20 unit (with the membrane of molecular weight cut-off 10 kDa) and centrifugation at 6000 x ***g*** (10ºC) for five minutes in the Heraeus multifuge X3R centrifuge. The filtrate concentrates were collected for protein assays and gus assays

Cell pellets re-suspended in 3 ml gus extraction buffer (pH 7) were disrupted by sonication for 3 x 30 seconds on ice (70-74% power) with one-minute intervals on ice. The crude cell extracts were examined for cell lysis under the light microscope (Leica) to ensure the disruption of the majority of cells. 0.2 ml crude cell extract was collected for gus assays.

2.8 ml of crude cell extracts were centrifuged at *25000 x* ***g*** (4ºC) for 30 minutes to sediment cell debris. The supernatant (contain soluble proteins) was collected for protein assay. The sediment membranous fractions (contain insoluble protein) solubilised with 2.8 ml of 1 M sodium hydroxide solution for 16 h at -20ºC. After 16 h, samples were thawed on ice, boiled for 10 minutes and collected for protein assay.

Gus assays and determination of total gus yield

Gus assays were performed on the filtrate concentrates and crude cell extracts samples prepared as described. Gus assays on 4-nitrophenyl β-D-glucuronide and the spectrophotometric measurement at 405 nm of the product (4-nitrophenolate) were performed as described by Jefferson [58-60] Total gus activity was determined as the sum of the enzyme activity measured in crude cell extracts and in filtrate concentrates. A unit of gus is the amount of the enzyme that catalyses the formation of one nanomole of product per minute at 37ºC, allowing total gus activity to be converted into total enzyme units. According to Jefferson [59], one unit of gus at 37ºC and pH 7 was approximately 5 ng of pure *β*-glucuronidase [58]. The total amount of gus was therefore estimated by multiplying the total units of gus by 5 ng. Total gus yield was determined as the total amount of gus per dry cell weight (ng gus/g dry cell weight).

Biorad protein assay and determination of total protein yield

Biorad protein assays were performed on the filtrate concentrates, crude supernatants and the solubilised membranous fractions prepared as described in the previous section. Assays were performed following the instructions of the manufacturer (Biorad). Total protein concentration was determined as the sum of protein concentration in the soluble fractions, insoluble fractions and in the extracellular medium. Total protein yield was determined as the total amount of protein per dry cell weight (mg protein/g dry cell weight).

Measurement of acetate consumption and determination of specific acetate uptake rate

Acetate consumption during growth was determined using the MegaEnzymes Ltd protocol for the acetic assay kit. The specific acetate uptake rate was measured as functions of acetate consumption, the specific growth rate of culture and culture density [62]. Specific acetate uptake rates were determined for heterotrophic and mixotrophic cultures growing in TAP medium.

Measurement of photosynthetic activity and determination of the specific photosynthetic rate

Measurement of photosynthetic rates was performed by the oxygen electrode method using instructions of the DW2 oxygen electrode manufacturer (Hansatech Instruments Ltd). The specific photosynthetic rate is taken as specific CO_2 fixation rate (assuming photosynthetic quotient of 1) was estimated by dividing the photosynthetic rate with the culture density. Specific CO_2 fixation rate was determined for autotrophic and mixotrophic cultures in µmol CO_2 fixed per g dry cell weight per hour.

Estimating recombinant gus protein burden (protein cost)

The protein cost was estimated as the fractional reduction in specific growth rate due to the expression of recombinant gus in the strain, using equation 2 adapted from Malakar and Venkatesh [22]:

$$Cost = \left(\frac{\mu_{max\ (TRANSGENIC)} - \mu_{max\ (CONTROL)}}{\mu_{max\ (CONTROL)}} \right) \quad (2)$$

where μ_{max} is the maximum specific growth rate determined at the exponential growth phase. *CONTROL* is the control strain (Bam10::cc373 mt+) lacking gus expression, and *TRANSGENIC* is the gus expressing strains (Gus12-2 and Gus12-B).

Determination of cellular ATP concentration

The cellular ATP concentration was determined by the luciferin-luciferase bioluminescence reaction method [63] and following the instructions of the ATP bioluminescence assay kit CLS II manufacturer (Roche Diagnostics GmbH, Germany).

FBA Modelling Methodology

Flux balance analysis (FBA), a constraint-based reconstruction and analysis (COBRA) method, was used to simulate metabolism using the cobra toolbox [42] freely available at http://opencobra.sourceforge.net/ in the MatLab environment. The Cobra toolbox includes a linear programming solver (glpk), and a number of code sources for the analysis and simulation of models based on the system biology markup language (SBML) [42]. The validated SBML model, AlgaGEM [49] was downloaded from http://www.biomedcentral.com/1471-2164/12/S4/S5. The commands for executing cobra scripts and the scripts for running FBA simulations on the SBML model are described and provided in Supplementary M1 (1.1)

Basic concepts of FBA method:

In FBA the metabolic network is described in terms of its stoichiometric matrix ***N***, which summarizes in a computationally-friendly way the metabolites and metabolic reactions occurring in the system. The time evolution of the metabolite concentrations in the network is expressed as the product of the stoichiometric matrix ***N*** and the vector of reaction fluxes [64] v, according to equation (3):

$$\frac{dC}{dt} = N.v \quad (3)$$

where, C denotes the column vector of metabolite concentrations, and v the column vector of the fluxes. In FBA formulation, equation 3 is equated to zero in order to constrain the system to a steady-state condition. At steady-state, each metabolite is produced at the same rate as it is consumed so no net accumulation occurs (equation 4):

$$\frac{dC}{dt} = N.v = 0 \quad (4)$$

Other constraints are introduced in FBA to define (if known) the maximal flux capacity of each reaction (equation 5):

$$v_j^L \leq v_j \leq v_j^U \quad (5)$$

where, v_j^L and v_j^U are the lower and upper bound respectively of the reaction flux v_j. The constraints expressed in equation 5 are also used to define the directionality of the different reactions (for example, if $v_j^L = 0$, and $v_j^U \neq 0$, then reaction j can only occur in the positive direction). Equations 4 and 5 define a linear problem in the variables, v. Any solution v, of such problem, represents a theoretically possible steady-state flux distribution through the underlying metabolic network. Since there are generally more reactions than metabolites in genome-scale metabolic networks [35, 38], the problem defined by Equations 4 and 5 become underdetermined i.e. it has an infinite number of solutions. The entire collection of solutions is referred to as the null-space of N and represents the phenotype of the network [35, 38] However, not all the mathematically possible solutions are biologically relevant [35]. In order to identify one solution that is biologically more representative than the others, FBA relies on the assumption that biological systems have evolved to optimize specific biological processes. FBA formalizes this assumption through the introduction of an objective function [35], *f.* The objective function is a mathematical expression that represents the criterion of optimality assumed to be fulfilled by the cell, for example, production of biomass, or ATP, or protein production). The basic formulation of an FBA problem is then given by equation (6) [35]:

Maximize $f := \mathbf{c}^{\mathrm{T}} . \mathbf{v}$

Subject to

$\boldsymbol{N}. \mathrm{v} = 0$

$$v_j^L \leq v_j \leq v_j^U \quad (6)$$

where, the objective function *f*, to be maximized takes the form of linear combinations of the flux variables $\boldsymbol{v}$ with coefficients $\boldsymbol{c}$. In other terms, the different fluxes $\boldsymbol{v_j}$ contribute to the objective

function *f* with weights given by the coefficients c_j. Equation 6 is an instance of a class of problem called linear programming (LP) problems [35]. Today, there are a number of efficient algorithms that solve the LP problems using the accessible and low-cost computing power of common laptops. An FBA solution is an optimal solution of the LP problem as expressed in equation (6). The FBA solution is a flux distribution, *v* that maximizes the objective function *f* while satisfying the steady-state condition and the constraints imposed on the individual fluxes in equation (6) [35]. For example, in order to predict the maximal theoretical yield of recombinant gus protein in microalgae, and to identify an optimal flux distribution leading to such yield, we can define the objective function *f* to represent the production of gus. The maximal yield of the gus protein will then be given by the maximized value of the objective function (*f*), and the flux distribution is given by the corresponding FBA solution *v*. The FBA predicted gus yield was compared with the experimentally measured gus yield to test the model prediction. The model was further refined with experimental data (constraints) where needed, to get the predictions that are compatible with experimental observations.

Adding gus production reaction to AlgaGEM

A reaction accounting for the production of the gus protein was added to the model as shown in equation 7. The commands and scripts for adding and executing this adaptation are described and provided in Supplementary M1 (1.1).

$$A.A. + tRNA + GTP \longrightarrow P + tRNA + GDP + pi \quad (7)$$

In the simple representation of equation 7, *A.A* refers to amino acids, *tRNA* refers to transfer RNA, *GTP* refers to guanine nucleotide trisphosphate. In the model representation, amino acids are substrates, GTP (energy source) and tRNA transfer each amino acid into the protein. The products are shown on the right-hand side of equation 7. *P,* refers to the recombinant protein (gus), *GDP* and *pi* refer to guanosine diphosphate and inorganic phosphate respectively. The *tRNA* on the right-hand side of equation 7 is the unbound tRNA after an amino acid is added to the protein. The addition of an amino acid into protein requires one tRNA and one GTP hydrolysis. The reaction in equation 7 is a lumped reaction that acts as a demand for the correct amounts of tRNAs, amino acids, and GTP in the production of gus protein. The objective function was defined as the flux through the gus production reaction (equation 7). The criterion of optimality was then set as the maximization of such flux.

Other constraints on the model

To perform FBA simulation of gus protein production in the model, experimentally measured fluxes for carbon and light uptake were constrained on the model in the different growth conditions. The FBA constraints in autotrophic, heterotrophic and mixotrophic conditions are provided in Supplementary information M1 (1.2).

3. RESULTS AND DISCUSSION

The compositions of TAP and minimal media used for growing the *C. reinhardtii* cultures are shown in Supplementary information M2 (2.1). Minimal media was used for autotrophic growth in continuous light condition at 54 µmol photons/m^2/s. TAP media was used for heterotrophic growth in continuous dark condition, and for mixotrophic growth in continuous light at 54 µmol photons/m^2/s. The results characterizing the growth of the cultures under autotrophic, heterotrophic and mixotrophic conditions are presented in Table 1.

Table 1: Maximum specific growth rate (μ_{max}) was determined from the linear slope of the plot of the natural logarithm of culture density against time during exponential growth phase 24-96 h for autotrophic and heterotrophic cultures, 24-72 h for mixotrophic cultures). Protein cost was calculated according to equation 2 and expressed as a percentage reduction of the growth rate. Recombinant gus protein yield, total protein yield, and cellular ATP concentrations were measured for 72 h cultures at exponential growth phase. Specific acetate uptake rates and specific.

		***C. reinhardtii* strains**		
		Bam10::cc373mt+	**Gus12-2**	**Gus12-**
Heterotrophic condition	**Mean maximum specific** growth rate (10^{-2} h^{-1})	2.90 ± 0.01	2.42 ± 0.02	2.45 ± 0.04
	Mean gus yield (ng gus/g dry wt) x 10^{-5}	0	2.66 ± 0.45	2.62 ± 0.75
	Mean total protein yield (mg protein/g dry wt)	472 ± 12	493 ± 61	471 ± 22
	Mean protein cost (%)	0	-16.5 ±	-15.5 ±
	Mean cellular ATP (mM)	0.15 ± 0.01		-
	Mean specific acetate uptake rate (mmole acetate consumed/g dry wt/h)	1.61 ± 0.17	1.71 ± 0.29	-
Autotrophic condition	**Mean maximum specific growth rate** (10^{-2} h^{-1})	3 ± 0.2	3.1 ± 0.3	3.08 ± 0.2
	Mean gus yield (ng gus/g dry wt) x 10^{-5}	0	3.2 ±	3 ± 0.37
	Mean total protein yield (mg protein/g dry wt)	569 ± 96	511 ± 39	554 ± 38
	Mean protein cost (%)	0	3.3 ± 4.0	0.6 ± 4.8
	Mean cellular ATP (mM)	0.31 ± 0.03		-
	Mean specific CO_2 fixation rate (mmole CO_2 fixed/g dry wt/h)	11.09 ± 0.73	11.74 ± 0.22	-

Mixotrophic condition	**Mean maximum specific growth rate** (10^{-2} h^{-1})	5.75 ± 0.1	5.73 ± 0.1	5.87 ± 0.04
	Mean gus yield (ng gus/g dry wt) x 10^{-5}	0	3.75 ± 0.71	3.63 ± 0.18
	Mean total protein yield (mg protein/g dry wt)	629 ± 35	603 ± 37	577 ± 21
	Mean protein cost (%)	0	-0.3 ± 4.4	2.1 ± 3.9
	Mean cellular ATP (mM)	0.21 ± 0.03	-	-
	Mean specific acetate uptake rate (mmole acetate consumed/g dry wt/h)	1.08 ± 0.1	1.03 ± 0.07	-
	Mean specific CO_2 fixation rate (mmole CO_2 fixed/g dry wt/h)	7.99 ± 0.69	-	-

photosynthetic rates were determined for 72 h cultures at exponential growth phase. The mean and standard deviation values were determined for six biological replicates and two technical replicates each. Cultures were propagated in shake flasks at constant 25ºC and 90 rpm in media under autotrophic, heterotrophic and mixotrophic conditions.

The growth of cultures was reflected by the increase in cell numbers with time. The growth curves in autotrophic, heterotrophic and mixotrophic conditions are presented in (Supplementary information M2 (2.2a – 2.2c). Growth rates were compared in terms of the maximum specific growth rate under autotrophic, heterotrophic and mixotrophic conditions. The maximum specific growth rate was determined during the exponential growth phase from the slope of the linear plot of the natural log of cell density against time. Our results (Table 1) show that cultures grown in heterotrophic condition presented the lowest growth rates. The highest growth rates occurred in mixotrophic condition. Limitations to the growth of cultures in heterotrophic conditions included lack of light, depletion of acetate (sole carbon and energy source), and high rise in pH (Supplementary information M2 (Figure 2.3a). Heterotrophic cultures were observed to run out of acetate through consumption of the substrate, exhibit rapid rise in pH, and attained stationary phase after about 144 – 168 h followed by death phase. As a consequence, heterotrophic cultures achieved lowered final cell density, typically ~3 - 4 million cells/ml and shorter longevity.

The growth rate of cultures in autotrophic condition was higher than in heterotrophic condition. Our result suggests photosynthetic growth fuelled by light is more optimal than growth fuelled by acetate metabolism (fermentation) for *C. reinhardtii* cultures. However, compared to mixotrophic cultures the autotrophic cultures have significantly reduced growth rates. The reduction in growth rate may be due to the lack of organic carbon in the minimal media used for autotrophic cultures, whereas, acetate served as additional carbon and energy source for growth in mixotrophic condition. The main feature with autotrophic and mixotrophic cultures were the attainment of very much higher

cell densities (> 10 million cells/ml). Additionally, culture growth and longevity persisted for much longer periods e.g. autotrophic cultures (>30 days) and mixotrophic cultures (>20 days) under continuous light conditions at 54 µmol photons/m^2/s.

No growth was observed for cultures grown in the dark in the acetate-free media such as minimal media (Supplementary information M2 (Figure 2.2d). However, the inclusion of acetate in growth medium e.g. TAP supported the growth of cultures in the dark, highlighting the strict requirement for acetate in the dark condition. Growth was observed in the acetate-free media supplied with light, indicating the availability of light to be another requirement for growth. No growth was observed for cultures propagated in nitrogen-free media such as the ammonium-free medium (Supplementary information M2 (Figure 2.2e). Ammonium is the sole nitrogen source in TAP and minimal media growth of *C. reinhardtii* cultures, and thus availability of ammonium is another factor that strictly affects the growth of cultures. This study identified limiting factors to the growth of cultures to include the availability of light, availability of carbon and nitrogen substrates, and pH of media. The optimum pH for growth of *C. reinhardtii* was found to be about pH 7.30. The growth of cultures in heterotrophic condition was most affected and limited by these factors. Growth experiments were performed to identify strategies that may be used effectively to reduce the limitations, particularly, the limitations of heterotrophic cultures to significantly improve the cell density achievement and longevity of heterotrophic cultures.

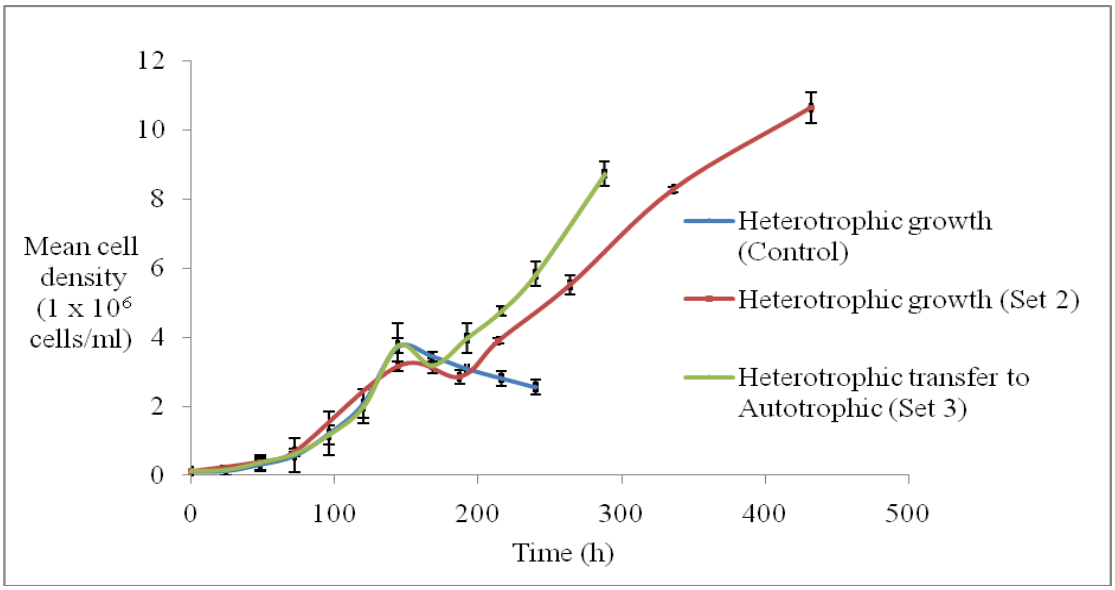

Figure 1: Heterotrophic growth of Gus12-2 cultures (control), (Set 2) and (Set 3 experiments). The mean cell density and standard deviation values were determined from three biological and two technical replicates each.

In each experiment, the acetate concentration in the media was determined using the acetic acid assay method. In the first set of experiments which we called CONTROL (blue line, Figure 1), the heterotrophic cultures were grown in TAP. Growth was measured and the cultures reach the

stationary phase at about 144 h (0 mM acetate) with a rise in culture pH ~0.7 from initial pH 7.30. The final cell density was ~3.7 million cells per ml, and the acetate-depleted cultures subsequently entered the death phase as seen in Figure 1.

In the second set of an experiment which we called SET 2 (red line, in Figure 1), the heterotrophic cultures were grown in TAP. At stationary phase (144 h), acetate in the media was 0 mM and the final cell density was ~ 3.2 million cells/ml. The acetate-deplete cultures were allowed to enter death phase. At 187 h (pH 8.4) the culture density decreased to ~ 2.8 million cells/ml, was harvested by low-speed centrifugation, washed twice with reverse osmosis water, and transferred into new sterile TAP buffered at pH 7.30. The cultures were incubated in the dark with the resumption of growth observed as in Figure 1. The growth was monitored, and at different times: 264, 336 and 432 h respectively, the cultures were harvested, washed and re-transferred into new TAP medium buffered at pH 7.30 and propagated in heterotrophic condition. Using this strategy, significant improvements in growth and culture longevity was observed for the heterotrophic cultures. The measured cell densities at 187, 264, 336 and 432 h were 2.8, 5.5, 8.3, and 10.7 million cells per ml respectively. By supplying exogenous substrates (in TAP media) into the carbon-depleted cultures, and provision of effective buffering of the medium around pH 7.30, cultures in heterotrophic condition achieve very high growth (high cell density) and longevity that was comparable to autotrophic and mixotrophic cultures. The significance of the result was the possibility to revive dying cultures or cultures in death phase into actively growing cultures through transferring into media rich in nutrients (e.g. acetate, ammonium) and adequate buffering of pH around the optimum 7.30. After 432 h (18 days) in the heterotrophic condition, the growth of heterotrophic cultures was pronouncedly sustained with at least a 3.4-fold increase in the measured cell density.

In the third experiment which we called SET 3 (green line, in Figure 1), the heterotrophic cultures in were grown in TAP. The final cell density at the stationary phase (144 h) was ~3.7 million cells/ml and acetate concentration in the media decreased to 0.0 mM. The cultures were allowed to enter the death phase. At 168 h (pH 8.2), the culture density declined to ~3.2 million cells/ml. The cultures were transferred from the dark condition and supplied continuous light at 54 µmol photons/m^2/s. Following the supply of light, cultures were observed to resume growth within 24 hours (Figure 1). The resumption of autotrophic growth was rapid and the culture density increased to ~8.7 million cells/ml within a 120 h interval. In addition, the pH of the medium was observed to decrease from pH 8.2 to pH 7.7 within the time interval covering the resumption of autotrophic growth. Significantly, our result shows that heterotrophic in death phase could be revived and made to resume growth by transferring the cultures to light, in this case into the high growth of autotrophic cultures. The autotrophic growth favoured a pH decrease towards the more optimal pH. The transfer to light afforded the supply of free energy for photosynthetic growth, with the cells resorting to using CO_2 in the flask (or dissolved in the medium) as the sole carbon source for growth and cell

maintenance. In Table 1, the results of recombinant gus and total protein yields determined for the cultures grown in autotrophic, heterotrophic and mixotrophic conditions are presented. The yield values were determined from cultures during the exponential growth phase (72 h), a period characterized by the rapid but steady increase in growth and doubling of cell numbers. Heterotrophic cultures have the lowest recombinant gus and total protein yields amongst the three conditions compared. Recombinant gus and total protein yields were highest in the mixotrophic cultures while autotrophic cultures had yields intermediate between those of mixotrophic and heterotrophic cultures. The heterotrophic condition was one that limited recombinant gus and protein productivity the most for growing cultures. The protein cost was analysed across the three growth conditions using the formalism of equation 2 and expressed as a percentage value in Table 1. For the analysis, the maximum specific growth rates of the gus expressing strains (Gus12-2 and Gus12-B), and the control strain (Bam10::cc373 mt+) which do not express recombinant gus were compared. When compared in heterotrophic condition, the mean values of maximum specific growth rates of Gus12-2 and Gus12-B were significantly different from the mean value of maximum specific growth rates for Bam10::cc373 mt+ ($p = 0.003$) at 95% confidence. Gus12-2 and Gus12-B heterotrophic cultures of show high protein cost for the expression of recombinant gus i.e. the maximum specific growth rates of Gus12-2 and Gus12-B cultures were reduced by about 16 - 17% compared to the maximum specific growth rate of Bam10::cc373 mt+. However, for autotrophic or mixotrophic Gus12-2 and Gus12-B cultures, there were no significant differences in the mean values of their maximum specific growth rates and that of the Bam10::cc373mt+ counterparts. Consequently, there was no reduction in growth rates of Gus12-2 and Gus12-B expressing recombinant gus compared to Bam10::cc373 mt+ in autotrophic or mixotrophic conditions. The analysis of protein cost under the two conditions presented no detectable protein cost and large standard deviation values reflecting the wide variability of the data. These results show that protein cost was significant for heterotrophic cultures, representing stress condition for growing cultures and expression of recombinant gus. With cultures constrained to use only acetate (a limited substrate) for carbon and energy requirements, heterotrophy presented the most limiting conditions for growth and protein production in terms of lower growth rates, lower protein yield and productivity. The expression of recombinant gus reduced growth rates further in Gus12-2 and Gus12-B. On the other hand, autotrophic and mixotrophic conditions presented more optimal conditions for growth and protein production. In both conditions, photosynthetic growth was fuelled through utilizing light (an unlimited energy source) and respired CO_2 [65, 66], as a carbon source for growth [63, 64]. Mixotrophic cultures used acetate as additional carbon and energy source. The result for autotrophic and mixotrophic cultures were high growth rates, higher protein yield, and productivity. The expression of recombinant gus did not reduce the growth rates.

The cellular ATP concentration may be used as an indicator of the free energy available for growth

and cell maintenance. The total cellular ATP concentration of cultures was determined during the exponential growth phase of the cultures using the ATP bioluminescence assay. The total cellular ATP concentration was highest in autotrophic cultures ~0.31 mM while the lowest was in heterotrophic conditions ~0.15 mM. The total cellular ATP concentration of mixotrophic cultures was ~0.21 mM. Total cellular ATP concentration was significantly different across the three growth conditions compared suggesting ATP balances from metabolisms in the three conditions may be different. In Bam10:cc373 mt+ cultures, the difference in mean total cellular ATP concentration was significant between autotrophic and heterotrophic ($p = 0.001$), between autotrophic and mixotrophic conditions ($p = 0.02$), and between the mixotrophic and heterotrophic conditions ($p = 0.02$) at 95% confidence. Compared with previous reports, the total cellular ATP concentration was consistent with the values reported by Rebeille and Gans [67] for the photosynthetic mutant strain of *C. reinhardtii* grown in heterotrophic condition [67]. However, no reports on measurements of total cellular ATP concentration in *C. reinhardtii* in autotrophic or mixotrophic conditions exist. Nonetheless, our result suggests that heterotrophic condition may be one that is energetically more-limited in terms of a lowered total cellular ATP concentration i.e. one with a lower ATP balance from metabolisms. Autotrophic and mixotrophic cultures receive an unlimited supply of energy (light) and convert solar energy into chemical energy (ATP) through photosynthetic phosphorylation of ADP. Besides, the ability to fix CO_2 into sugars provide intermediates for the biosynthesis of energy storages such as starch and carbon for intermediary metabolisms, the extra incentives for producing cellular materials and growth. In heterotrophic condition, acetate is the only carbon and energy source hence cells may be limited in the amount of ATP molecules that could be generated from acetate metabolism. Moreover, acetate may be expected to have some uncoupling effect on cell membranes and extra energy (ATP) must be used by cells to reduce this effect. Therefore, the cellular ATP concentration may be higher in autotrophic and mixotrophic cultures than in heterotrophic cultures. However, mixotrophic cultures exhibit a mix of autotrophic growth in light and heterotrophic growth on acetate. Though cellular ATP concentration is highly regulated in cells [65], the total cellular ATP concentration in mixotrophic cultures may represent an average ATP balance for the complex mix of metabolisms arising from autotrophic and heterotrophic growth. The utilization rate of carbon substrates such as specific uptake rate of acetate in heterotrophic and mixotrophic conditions, specific photosynthetic rate (specific CO_2 fixation rate) in autotrophic and mixotrophic conditions was determined during exponential phase (Table 1) and used as rough estimates of carbon fluxes into cells. On the basis of carbon moles, the estimated total carbon flux in mixotrophic condition (~10 mmoles carbon/g dry wt/h) and autotrophic condition (11 mmoles carbon/g dry wt/h) were higher than in heterotrophic condition (~3 mmole carbon/g dry wt/h). The growth of cultures, recombinant gus, and total protein production may be limited more in heterotrophic cultures than in autotrophic or mixotrophic cultures, by a shortfall in carbon flux into

cells.

Modelling results and Discussions:

A good strategy to optimize recombinant protein production in *C. reinhardtii* would be one that increased the culture density (so that a higher number of cells expressed the target protein) or one that increased the yield of the target protein in each cell. FBA modelling was used to study steady-state fluxes distributions in the *C. reinhardtii* metabolic model (AlgaGEM), and indeed to identify a flux pattern that maximizes gus production (Table 2) and gus yield (Table 3) under the given set of FBA constraints. The FBA simulation of gus production was performed for the heterotrophic, autotrophic and mixotrophic growth conditions with ammonia as nitrogen source.

Table 2: FBA predicted optimal steady-state flux for maximal gus production in heterotrophic, autotrophic and mixotrophic FBA simulations. Experimentally determined values for specific acetate uptake rates, specific CO2 fixation rates calculated as total carbon fluxes and used to constrain the FBA simulation of autotrophic, heterotrophic and mixotrophic conditions of the model.

Condition	Carbon substrate	Total carbon flux through network (mmole carbon/g dry wt/h)	FBA optimal steady-state flux for maximal gus production (mmole gus /g dry wt/h) x 10^{-4}
Heterotrophic	Acetate	3.4	5
Autotrophic	CO_2	11	19
Mixotrophic	Acetate and CO_2	10	23

Based on the optimal steady-state flux distribution predicted by FBA for gus production (Table 2), the FBA gus protein yields were calculated according to equation 8 with units of mmole gus per mmole carbon:

$$Y_{Protein} = \left(\frac{Predicted\ optimal\ flux\ for\ maximal\ gus\ production}{Total\ carbon\ flux} \right) \qquad (8)$$

here, $Y_{Protein}$ is the FBA gus yield (mmole gus/mmole carbon). The numerator is the FBA predicted optimal flux for maximal gus production (mmole gus/g dry wt/h), and the denominator is the total uptake flux of carbon-containing nutrients (mmole carbon substrate/g dry wt/ h). The carbon substrate was acetate in heterotrophic condition; CO_2 in autotrophic condition; and acetate and CO_2 in mixotrophic condition. The FBA gus yield was then expressed in terms of carbon yield of gus

according to equation 9:

$$Y_C = Y_{Protein} * \left(\frac{number\,of\,moles\,of\ carbon\,in\,gus\,protein}{number\,of\,moles\,of\,carbon\,in\,substrate} \right) \quad (9)$$

where Y_C is the carbon yield of gus expressed as g carbon in gus per g total carbon. Gus is a tetramer protein [68], with each subunit ~68 kDa protein and 603 amino acid residues make up gus protein sequence composition [58]. There are 3068 moles of carbon atoms per gus protein sequence composition (Supplementary M3 (Table 2). The predicted FBA gus yield in heterotrophic, autotrophic and mixotrophic conditions are presented in Table 3.

Table 3: FBA gus yield and recombinant gus yield from growth experiments. The mean of experimentally measured recombinant gus yield and standard deviation values were determined from six biological replicates and two technical replicates each from Gus12-2 in heterotrophic, autotrophic and mixotrophic conditions. For comparison with the FBA gus yield, the experimental gus yield in units of g gus protein per g dry cell weight were converted into units of g carbon in gus per g total carbon (Supplementary M3 (3.4)).

Condition	FBA yield (g carbon in gus/g total carbon)	Mean Experimental yield ± sd (g gus protein/g dry cell wt) x 10^{-4}	Mean Experimental yield ± sd (g carbon in gus/g total carbon) x 10^{-4}
Heterotrophic	0.451	2.66 ± 0.45	2.10 ± 0.36
Autotrophic	0.530	3.20 ± 0.69	2.53 ± 0.55
Mixotrophic	0.700	3.75 ± 0.71	2.96 ± 0.56

The experimentally determined recombinant gus yields were much lower than the FBA gus yield (Table 3). Nonetheless, the predictions were consistent in qualitative and relative terms with the experimental gus yields for the three growth conditions. The FBA gus yield was lowest in the heterotrophic condition but highest in mixotrophic condition. The FBA gus yield was higher in autotrophic than heterotrophic condition, confirming with experiments that heterotrophic condition was the most limiting for gus production. However, FBA predictions could be made to approximate more closely to biologically relevant values for gus yield, if all the possible biological constraints represented by values for all external and internal fluxes for all nutrients uptake, intermediary metabolisms, product secretions etc could be measured and applied directly as constraints into the

FBA modelling. The simulations for FBA gus yields in the 3 conditions were routinely reproducible, allowing analysis of FBA predicted steady-state fluxes in the network in the 3 conditions. Translation or protein synthesis was reported as the major hierarchical regulator of protein yield in *C. reinhardtii* [69, 70]. Thus we chose to analyse the predicted amino acids total steady-state flux distributions in the network. The total steady-state flux of each amino acid was given by the summation of two combinations (amino acid flux diverted towards gus production, and the amino acid flux diverted towards biomass formation). The steady-state fluxes of amino acid towards gus production and amino acid steady-state fluxes for biomass formation in the FBA simulation of autotrophic, heterotrophic and mixotrophic conditions are presented Supplementary M3-(Tables 3.3a – 3.3c). Since heterotrophy was the condition that limited gus production the most, our analysis focused on the example to identify and understand how the amino acids steady-state fluxes affected heterotrophic FBA gus yields.

Table 4: Amino acid steady-state fluxes predicted by FBA under the heterotrophic condition, and the abundance of each amino acid in the gus protein sequence composition. The gus protein sequence composition [58] is provided in Supplementary M3-(Figure 3.2a and Table 3.2b).

Amino acids	Letter symbol	Number of amino acid residues in gus composition	Amino acid total steady-state flux (mmole/g dry wt/h) x 10^{-6}
Cysteine	C	9	767.164
Methionine	M	13	1108.126
Histidine	H	19	1619.568
Tryptophan	W	19	1619.568
Proline	P	24	2045.771
Tyrosine	Y	24	2045.771
Serine	S	25	2131.011
Phenylalanine	F	25	2131.011
Lysine	K	27	2301.492
Asparagine	N	28	2386.733
Isoleucine	I	29	2471.973
Arginine	R	29	2471.973
Glutamine	Q	32	2727.694

Threonine	T	35	2983.416
Glutamate	E	40	3409.618
Aspartate	D	40	3409.618
Leucine	L	40	3409.618
Alanine	A	46	3921.061
Glycine	G	46	3921.061
Valine	V	53	4517.744
TOTAL		**603 residues**	**51400**

The distribution of the amino acid total steady-state fluxes in heterotrophic condition is presented in Table 4. These steady-state fluxes are the result of the FBA simulations (calculation of steady-state fluxes). Here, the FBA was used to simulate maximized gus production at fixed growth flux. The abundance of amino acid residues in the protein sequences for gus[58] is also shown in Table 4. The amino acid list in Table 4 shows that some amino acids have high total steady-state flux rates e.g. alanine, glycine, and valine. These amino acids were the most abundant amino acids in gus composition with 46, 46 and 53 residues respectively. Some amino acids carry low total steady-state flux rates in the network e.g. cysteine, methionine, histidine, and tryptophan. These amino acids were among the least abundant in the gus composition (9, 13, 19 and 19 residues respectively), suggesting that the more abundant an amino acid is in protein composition, the higher is its steady state flux towards the protein production. To test this further, separate FBA was run to compare the flux distributions associated with the synthesis of two differentially expressed endogenous protein of *C. reinhardtii*. In particular, separate FBA simulations were performed to maximize the production of ribulose-1, 5-bisphosphate carboxylase/oxygenase (rubisco) on the one hand, and ferroxidase on the other hand. Rubisco is a highly expressed protein in plants and algae [71] and ferroxidase is one of the low expressed endogenous protein in *C.* reinhardtii [72]. The protein sequence composition of rubisco [73, 74] and ferroxidase [75] is on Supplementary M3-(Figures 3.2a and 3.2b). The amino acid total steady-state fluxes predicted by FBA simulation of rubisco or ferroxidase production in heterotrophic condition are provided on Supplementary M3-(Table 3.2b)). With rubisco and ferroxidase examples, high total steady-state fluxes were found with the most abundant amino acids and low total steady-state fluxes with the least abundant amino acids for each protein composition. Based on the analyses of amino acid total steady-state fluxes, amino acids which carry low steady-state fluxes (limiting amino acids) and those that carry high steady-state fluxes in the network were identified. For example, for an amino acid on to be considered limiting the gus production, a flux threshold value of $\boldsymbol{\alpha}$ = 0.003 mmoles amino acid/g dry wt/h was introduced. Amino acid with a total

steady-state flux less than α was considered limiting, while amino acids with a total steady-state flux greater than α were considered non-limiting limiting. Based on this criterion, 14 amino acids were identified as limiting for gus. The 14 putative limiting amino acids for gus production were cysteine, methionine, histidine, tryptophan, proline, tyrosine, serine, phenylalanine, lysine, asparagine, isoleucine, arginine, glutamine and threonine (Table 4). Based on this analyses a new FBA simulation was performed this time allowing the uptake of 11 limiting amino acids (cysteine, histidine, tryptophan, proline, tyrosine, serine, phenylalanine, lysine, asparagines, isoleucine, and arginine) from the *in the silico* medium. Amino acids reported to be taken up *C. reinhardtii* cells from the growth media includes arginine [74, 75], proline [78], glutamine, leucine, isoleucine, lysine, serine, asparagines, alanine, valine, methionine, histidine and phenylalanine [79]. Another separate FBA simulation was then performed to include the uptake of 4 of such amino acids (arginine, leucine, proline, and glutamine). The FBA uptake rate for each amino acid was kept at -0.03 mmol/g dry wt/h in the two separate FBA. The FBA gus yield without uptake of amino acids (control), FBA gus protein yield for a model with the uptake of 11 limiting amino acids, and FBA gus yield for a model with the uptake of the 4 amino acids were compared in heterotrophic condition (Figure 2).

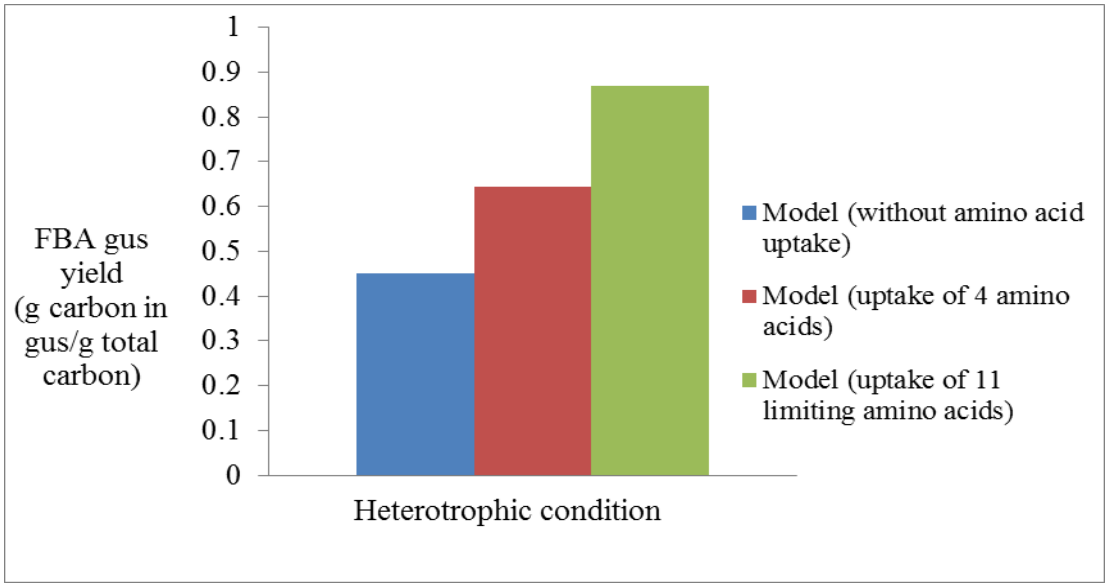

Figure 2: FBA predicted gus yield in heterotrophic condition for: (1) model without amino acid uptake, (2) model with uptake of the 4 amino acids (arginine, leucine, proline, glutamine), (3) model with uptake of 11 limiting amino acids (cysteine, histidine, tryptophan, tyrosine, serine, phenylalanine, lysine, asparagine, isoleucine, glutamine and threonine). In each of the 3 separate FBA simulations ammonium uptake was the main source of nitrogen.

The heterotrophic FBA gus yield was 0.451 g carbon in gus/g total carbon for the model without amino acid uptake (control). When the FBA simulation was performed with the uptake of the 4 amino acids (arginine, leucine, proline, and glutamine), the FBA gus yield was increased by ~1.44 fold to 0.65 g carbon in gus/g total carbon. For the FBA simulation with the uptake of the 11 limiting amino

acids, a 1.9 fold increase in FBA gus yield was observed (0.86 g carbon in gus/g total carbon). FBA predicted that significant increase in gus yield could be achieved by allowing the uptake of amino acids from *in silico* medium i.e. indicating amino acid limitations in the metabolic network. To rigorously verify the FBA predictions whether or not that recombinant gus yield in heterotrophic cells can be significantly increased by exogenous supply of the 11 limiting amino acids, or the four amino acids (arginine, leucine, proline, and glutamine), new sets of heterotrophic growth experiments were performed. In one set of experiments, the Gus12-2 strain was grown in TAP medium supplemented with the 11 limiting amino acids (cysteine, histidine, tryptophan, tyrosine, serine, phenylalanine, lysine, asparagine, isoleucine, glutamine, and threonine) each at 1 mM concentration. In the second set of growth experiments, the Gus12-2 strain was grown in TAP medium supplemented with arginine, proline, leucine, and glutamine (each amino acid at 1 mM concentration). In the third set of experiments that served as control, the Gus12-2 strain was grown in TAP medium without addition of amino acids. In each of the growth experiments, 9.35 mM ammonium chloride was the main nitrogen source in TAP medium. The recombinant gus yields were determined during the exponential growth phase of the heterotrophic cultures and presented in Figure 3. For comparison with the predicted FBA gus yield, the experimental gus yield values in units of g gus protein per g dry cell weight were converted into units of g carbon in gus per g total carbon (Supplementary M3 (3.4)).

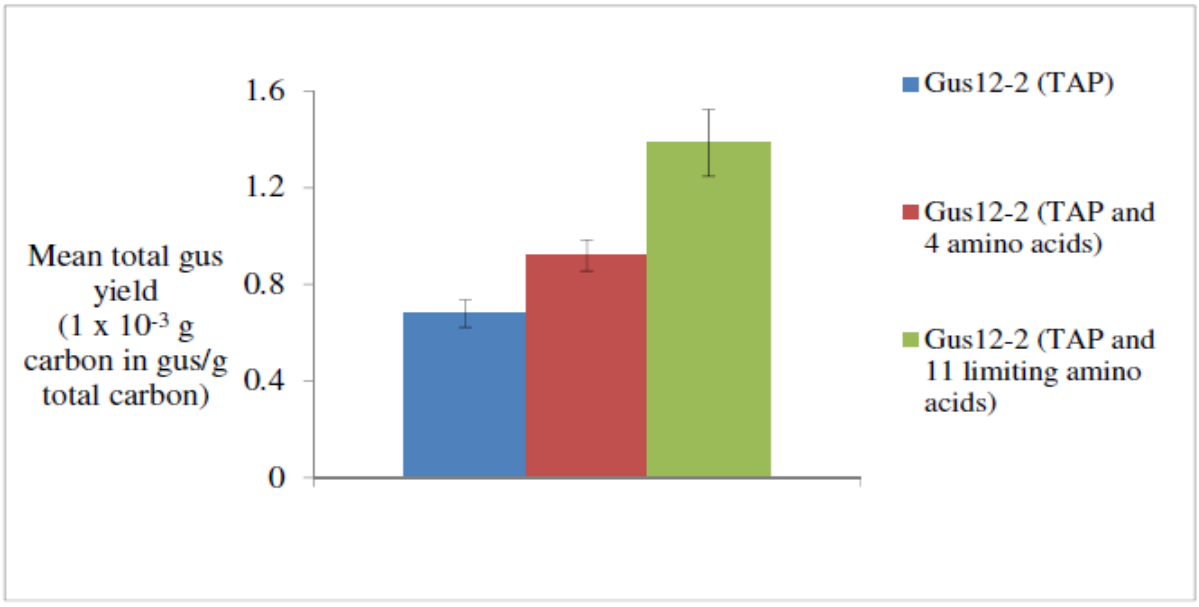

Figure 3: Recombinant gus yield (g carbon in gus/g total carbon) during exponential growth phase determined for heterotrophic Gus12-2 cultures grown: in TAP (control); in TAP containing four amino acids (arginine, proline, leucine and glutamine); in TAP supplemented with 11 limiting amino acids (cysteine, histidine, tryptophan, tyrosine, serine, phenylalanine, lysine, asparagine, isoleucine, glutamine and threonine). The mean and standard deviation values were determined from three biological and 2 technical replicates each.

The experimentally determined heterotrophic gus yields were ~0.70 x 10^{-3} g carbon in gus/g total carbon for the cultures grown in TAP (control), ~0.95 x 10^{-3} g carbon in gus/g total carbon for cultures grown in TAP supplemented with the 4 amino acids (arginine, proline, leucine and glutamine), ~1.42 x 10^{-3} g carbon in gus/g total carbon for cultures grown in TAP supplemented with the 11 limiting amino acids. These growth experiments verified that recombinant gus yield in heterotrophic cells can be significantly increased by exogenous supply of the 11 limiting amino acids, or the four amino acids (arginine, leucine, proline, and glutamine). Compared with the control cultures, a significant 1.36 fold increase in gus yield was observed when arginine, leucine, proline, and glutamine were supplied to the heterotrophic cultures. An even higher 2 fold increase was observed when the 11 limiting amino acids were supplied. A relatively similar and consistent trend observed with the FBA predictions. The result suggests a limitation of amino acid fluxes as a metabolic bottleneck for the recombinant gus production and yield. The identification of the limiting amino acid steady-state fluxes through FBA was used to inform the formulation of the growth medium to increase the experimental gus yield significantly. Since the FBA predictions were highly reproducible in growth experiments, next we focused to identify the effects of individual amino acid uptake to the FBA gus yield. Further FBA simulations and analysis were used to understand the effect that each amino acid uptake from the *in silico* has on the heterotrophic FBA gus yield. The first simulation, which was called FBA control, the FBA simulations for gus production was performed with ammonia uptake as the only nitrogen source. In all instances, the predicted heterotrophic gus yield for FBA control was 0.451 g carbon gus in gus/g total carbon. In the second FBA simulation, which was called model II, the uptake of ammonia and an amino acid uptake served as nitrogen sources. Here, the effect of the uptake of the amino acid on the FBA gus yield was analysed and compared with the gus yield of FBA control. The predicted effect of each amino acid uptake on the heterotrophic FBA gus yield in model II is listed in Table 5.

Table 5: Effect of amino acid uptake on heterotrophic FBA gus yield. The effect was expressed as a fold change. Fold change was calculated by dividing the FBA gus yield in the model II by FBA gus yield of the FBA control.

Amino acids	Heterotrophic FBA gus yield for model II with the uptake of ammonia and an amino acid (g carbon in gus/g total carbon)	Fold Change
Cysteine	0.463	1.027
Glycine	0.468	1.038
Histidine	0.472	1.048
Methionine	0.473	1.048

Serine	0.477	1.057
Alanine	0.479	1.062
Aspartate	0.481	1.066
Asparagine	0.483	1.070
Lysine	0.484	1.073
Threonine	0.485	1.075
Isoleucine	0.489	1.083
Glutamate	0.492	1.090
Tryptophan	0.493	1.091
Tyrosine	0.493	1.093
Glutamine	0.494	1.094
Proline	0.499	1.107
Valine	0.501	1.111
Arginine	0.502	1.113
Leucine	0.506	1.123
Phenylalanine	0.544	1.206

The yields in model II compared to the FBA control show the fold change. The uptake of ammonia and an amino acid increased the FBA gus yield in model II than if only ammonia was taken up as in the FBA control, confirming availability of amino acid as a metabolic bottleneck for the gus yield. In each FBA simulation for maximal gus production (objective function), gus production is a lumped reaction in the stoichiometric matrix that places the demand on amino acids. Some amino acids are made from ammonia, and if an amino acid is taken up with ammonia, this further increases the flux of the amino acid for gus protein production. Depending on the amino acid taken up, there was between 1.027 – 1.206 fold change in FBA gus protein yield (i.e. 2.7 – 20.6% increase in gus yields) for model II. By adding amino acid uptake individually to the FBA simulation, the predicted effect of each amino acid on gus yield was identified. This analysis enabled us to understand the effects that combinations of amino acids could have towards gus yield. For instance, in Table 5, the combined uptake of the 11 limiting amino acid on gus yield would be a summation effect for each of the 11 amino acids i.e. this sums to ~1.9 fold change (90% increase in gus yield) compared to the control. Similarly, the combined uptake of arginine, leucine, proline and glutamate uptake would be ~1.44 fold change (44% increase in FBA gus yield) compared to the control.

Amongst the 20 amino acids, uptake of phenylalanine provided the highest increase in FBA gus yield (~21%) while the uptake of cysteine contributed the least increase to FBA gus yield (2.7%). We observed that there are more abundant phenylalanine residues than cysteine residues in gus composition i.e. phenylalanine is required at higher total steady state flux than cysteine in the network (Table 4). Phenylalanine would be expected to be a better candidate amino acid that could be used to improve gus yield than would cysteine. The effect that an amino acid has on the FBA protein yield could also depend on the total number of carbon atoms contributed by the amino acid to the protein yield. The higher the total carbon atoms contributed, the higher will be the FBA yield. For example, glycine, alanine, aspartate (46, 46 and 40 residues respectively) are more abundant amino acids than phenylalanine (25 residues) in gus composition (Table 4). Yet, the uptake of phenylalanine contributes the highest increase to FBA gus yield than glycine, alanine or aspartate (Table 5). Each phenylalanine residue has 9 moles of carbon atoms, and thus a total number of 225 moles of carbon atoms are contributed by phenylalanine in the gus protein. From this, we find that, the uptake of phenylalanine results in a higher increase to FBA gus yield than glycine, alanine or aspartate that contribute 92, 138 or 160 moles of carbon atoms respectively in gus protein. The significance of Tables 4 and 5 highlights the importance and possibility to identify the effect of an amino acid uptake on the FBA gus yield. Upon understanding this effect, the knowledge could be used to design or formulate growth media for microalgae such as to increase recombinant gus yield expressed by the cells. Culture media may then be supplemented with the amino acid or combinations of amino acids that significantly increase the yield for the target protein. Though the sole nitrogen source in the media for growth was ammonium, cells are able to take up amino acids [74, 75, 79, 80]. Some amino acids are deaminated into 2-keto acids and ammonium before the ammonium is taken up into cells from the medium [79]. Such amino acids include asparagine, alanine, serine, isoleucine, lysine, glutamine, valine, leucine, methionine, histidine and phenyalanine [79]. The enzymes, L-amino oxidases, that catalyse the extracellular deamination of the amino acids have been characterized in *C. reinhardtii* [81, 82]. Two types of transporters in *Chlamydomonas* mediate the transport of ammonium into cells: a low-affinity high capacity transporter [83], and a high-affinity low capacity transporter [84, 85]. However, arginine is not deaminated extracellularly; rather a highly specific transport carrier was reported for the uptake of arginine into *C. reinhardtii* cells [76, 77]. It may be possible also, that other amino acids have yet to be identified transport carriers into cells. Then identifying the means by which amino acids enter into cells, optimizing the enzyme expressions (e.g. L-amino oxidases) or improving expressions for the specific carriers for amino acids into cells may be additional strategies to further increase recombinant gus yield in the cells. These remain aspects for future work, and indeed, should be exploited in the research aimed at increasing recombinant protein yield in the microalgae.

4. CONCLUSION

A challenge for recombinant protein production in microalgae is the inherent low yield of the proteins. Our study provided a platform to characterize the growth of *C. reinhardtii* and recombinant protein production in autotrophic, heterotrophic and mixotrophic growth conditions. The factors that limited the growth and recombinant protein production include the availability of light, availability of carbon and nitrogen substrates, pH changes, protein burden and energetic limitation (ATP). Of the three growth conditions, the heterotrophic condition was the most-limiting condition for growth and recombinant gus protein production with high protein cost. We identified the strategy that reduced the limitations and significantly increased the growth and longevity of heterotrophic cultures. This approach could be employed in fed-batch mode, is scalable and would allow high-titre culture density similar to those observed for autotrophic or mixotrophic cultures. In addition, FBA predictions and verifications were used to identify metabolic limitations of amino acids and strategies that increased the yield of recombinant gus in heterotrophic cells by 1.4 - 2 fold. The combination of the quantitative experiments, analysis and FBA modelling was a first in the research field for recombinant protein expression in microalgae. These approaches are transferable and applicable to other recombinant proteins expressed in the microalgae. Our work provides proof of concept that systems biology analysis of networked processes that affect protein production in cells, may help make protein production more predictable and contributes towards optimized production of recombinant proteins in microalgae.

ACKNOWLEDGEMENT

Oluwafemi Davies thanks the BBSRC, UK and EPSRC, UK for funding Doctoral Training programme in Systems Biology at the University of Manchester. Malkhey Verma thanks to the Central University of Punjab, Bathinda, India for seed grant funding in 2016.

CONFLICT OF INTEREST

Authors declare that they have no conflicting interests.

REFERENCES

1. Dove A. Uncorking the biomanufacturing bottleneck. Nat Biotechnol. 2002; 20: 777-779.
2. Fischer R, Liao YC, Hoffmann K, Schillberg S & Emans N, Molecular farming of recombinant antibodies in plants. Biol Chem. 1999; 380: 825-839.
3. Mayfield SP & Franklin SE. Expression of human antibodies in eukaryotic micro-algae. Vaccine. 2005; 23: 1828-1832.
4. Chebolu S & Daniell H. Chloroplast-Derived Vaccine Antigens and Biopharmaceuticals: Expression, Folding, Assembly and Functionality. Plant-Produced Microbial Vaccines. 2009; 332: 33-54.
5. Hiatt A, Cafferkey R & Bowdish K, Production of antibodies in transgenic plants. Nat. 1989; 342: 76-78.

6. Staub JM, Garcia B, Graves J, Hajdukiewicz PTJ, Hunter P, Nehra N, Paradkar V, Schlittler M, Carroll JA, Spatola L, Ward D, Ye GN & Russell DA. High-yield production of a human therapeutic protein in tobacco chloroplasts. Nat Biotechnol. 2000; 18: 333-338.
7. Franklin S, Ngo B, Efuet E & Mayfield S P, Development of a GFP reporter gene for *Chlamydomonas reinhardtii* chloroplast. Plant J. 2002; 30: 733-744.
8. Franklin SE & Mayfield SP, Prospects for molecular farming in the green alga *Chlamydomonas reinhardtii*. Curr Opin Plant Biol. 2004; 7: 159-165.
9. Ishikura K, Takaoka Y, Kato K, Sekine M, Yoshida K & Shinmyo A. Expression of a foreign gene in *Chlamydomonas reinhardtii* chloroplast. J Biosci Bioeng. 1999; 87: 307-314.
10. Mayfield, SP, Franklin SE & Lerner RA, Expression and assembly of a fully active antibody in algae. Proc Natl Acad Sci U S A. 2003; 100: 438-442.
11. Rasala BA, Muto M, Lee PA, Jager M, Cardoso RMF, Behnke CA, Kirk P, Hokanson CA, Crea R, Mendez M & Mayfield SP. Production of therapeutic proteins in algae, analysis of expression of seven human proteins in the chloroplast of *Chlamydomonas reinhardtii*, Plant Biotechnol J. 2010; 8: 719-733.
12. Ruf S, Karcher D & Bock R. 2007. Determining the transgene containment level provided by chloroplast transformation. ProcNatl Acad Sci U S A. 2007; 104: 6998-7002.
13. Gantar M & Svircev Z. Microalgae and cyanobacteria: Food for thought. J Phycol. 2008; 44: 260-268.
14. Ellstrand NC. When transgenes wander, should we worry? Plant Physiol. 2001; 125: 1543-1545.
15. Quist D. & Chapela IH. Transgenic DNA introgressed into traditional maize landraces in Oaxaca, Mexico. Nat. 2001; 414: 541-543.
16. Harris EH. *The Chlamydomonas Sourcebook: A Comprehensive guide to biology and laboratory use, (*New York, Academic Press, Inc.) 1989; vix 780.
17. Surzycki R, Greenham K, Kitayama K, Dibal F, Wagner R, Rochaix JD, Ajam T & Surzycki S. Factors effecting expression of vaccines in microalgae. Biologicals. 2009; 37: 133-138.
18. Komine Y, Kikis E, Schuster G & Stern D. Evidence for in vivo modulation of chloroplast RNA stability by 3 '-UTR homopolymeric tails in *Chlamydomonas reinhardtii*. ProcNatl Acad Sci USA. 2002; 99: 4085-4090.
19. Novick A & Weiner M, Enzyme induction as an all-or-none phenomenon. Proc Natl Acad Sci USA.1957; 43: 553-566.
20. Koch AL. The protein burden of lac operon products. J Mol Evol. 1993; 19: 455-462.
21. Dekel E & Alon U, Optimality and evolutionary tuning of the expression level of a protein. Nat. 2005; 436: 588-592.
22. Malakar P & Venkatesh KV. Effect of substrate and IPTG concentrations on the burden to growth of Escherichia coli on glycerol due to the expression of Lac proteins. Appl Microbiol Biotechnol.

2012; 93: 2543-2549.

23. Shachrai I, Zaslaver A, Alon U. & Dekel E. Cost of Unneeded Proteins in E. coil Is Reduced after Several Generations in Exponential Growth. Mol Cell. 2010; 38: 758-767.
24. Snoep JL, Yomano LP, Westerhoff HV & Ingram LO. Protein burden in zymomonas-mobilis - negative flux and growth-control due to overproduction of glycolytic-enzymes. Microbiol-UK. 1995; 141: 2329-2337.
25. Stouthamer AH. The search for correlation between theoretical and experimental growth yields. *Quayle, J R.* 1979; 21: 1-47.
26. Marr AG. Growth-rate of *Escherichia coli.* Microbiol Rev. 1991; 55: 316-333.
27. Dong HJ, Nilsson L & Kurland CG. Gratuitous overexpression of genes in *Escherichia coli* leads to growth-inhibition and ribosome destruction, J Bacteriol. 1995; 177: 1497-1504.
28. Lang G I, Murray A W & Botstein D, The cost of gene expression underlies a fitness trade-off in yeast. Proc Natl Acad Sci USA. 2009; 106: 5755-5760.
29. Dekel E, Mangan S & Alon U. Environmental selection of the feed-forward loop circuit in gene-regulation networks, Phys Biol. 2005; 2: 81-88.
30. Kalisky T, Dekel E & Alon U. Cost-benefit theory and optimal design of gene regulation functions, Phys Biol. 2007; 4: 229-245.
31. Snoep JL, Van Der Weijden CC, Andersen HW, Westerhoff HV & Jensen PR. DNA supercoiling in Escherichia coli is under tight and subtle homeostatic control, involving gene-expression and metabolic regulation of both topoisomerase I and DNA gyrase, Eur J Biochem. 2002; 269: 1662-1669.
32. Ter Kuile BH & Westerhoff HV. Transcriptome meets metabolome: hierarchical and metabolic regulation of the glycolytic pathway. FEBS Lett. 2001; 500: 169-171.
33. Kell DB & Westerhoff HV. Metabolic control-theory - its role in microbiology and biotechnology. FEMS Microbiol Lett. 1986; 39: 305-320.
34. Fell DA & Small JR. Fat synthesis in adipose-tissue - an examination of stoichiometric constraints. Biochem J. 1996; 238: 781-786.
35. Orth JD, Thiele I & Palsson BO. What is flux balance analysis? Nat Biotechnol 2010; 28: 245-248.
36. Papoutsakis ET. Equations and calculations for fermentations of butyric-acid bacteria, Biotechnol Bioeng. 1984; 26: 174-187.
37. Ranganathan S, Suthers PF & Maranas CD. OptForce: An Optimization Procedure for Identifying All Genetic Manipulations Leading to Targeted Overproductions. Plos Comput Biol. 2010; 6(4): e1000744.
38. Varma A, & Palsson BO. Metabolic flux balancing - basic concepts, scientific and practical use. Biotechnol. 1994; 12: 994-998.

39. Yang H, Roth CM & Ierapetritou MG. A Rational Design Approach for Amino Acid Supplementation in Hepatocyte Culture. Biotechnol Bioeng. 2009; 103: 1176-1191.
40. Lakshmanan M, Koh G, Chung BKS & Lee DY. Software applications for flux balance analysis. Brief Bioinform. 2014; 15: 108-122.
41. Becker SA, Feist AM, Mo ML, Hannum G, Palsson BO & Herrgard MJ. Quantitative prediction of cellular metabolism with constraint-based models: the COBRA Toolbox, Nat Protoc. 2007; 2: 727-738.
42. Schellenberger J, Que R, Fleming RMT, Thiele I, Orth JD, Feist AM, Zielinski DC, Bordbar, A, Lewis NE, Rahmanian S, Kang J, Hyduke DR & Palsson BO. Quantitative prediction of cellular metabolism with constraint-based models: the COBRA Toolbox v2.0, Nat Protoc. 2011; 6: 1290-1307.
43. Gevorgyan A, Bushell ME, Avignone-Rossa C & Kierzek AM. SurreyFBA: a command line tool and graphics user interface for constraint-based modeling of genome-scale metabolic reaction networks. Bioinformatics. 2011; 27: 433-434.
44. Hoppe A, Hoffmann S, Gerasch A, Gille C & Holzhuetter H G, 2011. FASIMU: flexible software for flux-balance computation series in large metabolic networks. BMC Bioinformatics. 2011; 12: 28.
45. Rocha I, Maia P, Evangelista P, Vilaca P, Soares S, Pinto JP, Nielsen J, Patil KR, Ferreira EC & Rocha M. OptFlux: an open-source software platform for in silico metabolic engineering. BMC Syst Biol. 2010; 4-45.
46. Grafahrend-Belau E, Klukas C, Junker BH & Schreiber F, FBA-SimVis: interactive visualization of constraint-based metabolic models. Bioinformatics. 2009; 25: 2755-2757.
47. Boele J, Olivier B G & Teusink B, FAME, the Flux Analysis and Modeling Environment. BMC Syst Biol. 2012; 6-8.
48. Boyle NR, & Morgan JA. Flux balance analysis of primary metabolism in *Chlamydomonas reinhardtii*. BMC Syst Biol. 2009; 3-4.
49. Dal'molin CGDO, Quek LE, Palfreyman RW & Nielsen LK. AlgaGEM - a genome-scale metabolic reconstruction of algae based on the *Chlamydomonas reinhardtii* genome. BMC Genomics. 2011; 12: S4-S5.
50. Duarte NC, Becker SA, Jamshidi N, Thiele I, Mo ML, Vo TD, Srivas R & Palsson BO. Global reconstruction of the human metabolic network based on genomic and bibliomic data. Proc Natl Acad Sci U S A. 2007; 104: 1777-1782.
51. Edwards JS, Ibarra RU & Palsson BO. In silico predictions of Escherichia coli metabolic capabilities are consistent with experimental data. Nat Biotechnol. 2001; 19: 125-130.
52. Mo ML, Jamshidi N & Palsson BO. A genome-scale, constraint-based approach to systems biology of human metabolism. Molecular Biosystems. 2007; 3: 598-603.

53. Shepherd HS, Boynton JE & Gillham NW. Mutations in 9 chloroplast loci of chlamydomonas affecting different photosynthetic functions. Proc Natl Acad Sci U S A. 1979; 76: 1353-1357.
54. Woessner JP, Masson A, Harris EH, Bennoun P, Gillham NW & Boynton JE. Molecular and genetic-analysis of the chloroplast atpase of *Chlamydomonas*. Plant Mol Biol. 1984; 3: 177-190.
55. Boynton JE, Gillham NW, Harris EH, Hosler JP, Johnson AM, Jones AR, Randolphanderson BL, Robertson D, Klein TM, Shark KB & Sanford JC. Chloroplast transformation in *Chlamydomonas* with high-velocity microprojectiles. Sci. 1988; 240: 1534-1538.
56. Gorman DS, Levine RP. Cytochrome f and plastocyanin: their sequence in the photosynthetic electron transport chain of *Chlamydomonas reinhardtii*. Proc Natl Acad Sci U S A. 1965; 45: 1665-1669
57. Day A & Goldschmidt-Clermont M. The chloroplast transformation toolbox: selectable markers and marker removal. Plant Biotechnol J. 2011; 9: 540-553.
58. Jefferson RA, Burgess, SM & Hirsh D. Beta-glucuronidase from *Escherichia coli* as a gene-fusion marker. Proc Natl Acad Sci U S A. 1986; 83: 8447-8451.
59. Jefferson RA, Assaying Chimeric Genes in Plants: The GUS gene Fusion System, Plant Mol Biol Report. 1987; 5: 387 - 405.
60. Jefferson RA, Kavanagh TA & Bevan MW. Gus fusions - beta-glucuronidase as a sensitive and versatile gene fusion marker in higher-plants. EMBO J. 1987; 6: 3901-3907.
61. Rochaix JD, Mayfield S, Goldschmidt-Clermont M & Erickson J, Molecular Biology of Chlamydomonas. *In:* SHAW, C. H. (ed.) Plant molecular Biology: a practical approach. (Oxford, England: IRL Press Ltd) 1988; p-313.
62. Manichaikul A, Ghamsari L, Hom EFY, Lin CW, Murray RR, Chang RL, Balaji S, Hao T, Shen Y, Chavali AK, Thiele I., Yang XP, Fan CY, Mello E, Hill DE, Vidal M, Salehi-Ashtiani K & Papin JA. Metabolic network analysis integrated with transcript verification for sequenced genomes. Nat Methods. 2009; 6: 589-U53.
63. Crouch SPM, Kozlowski R, Slater KJ & Fletcher J. The use of ATP bioluminescence as a measure of cell-proliferation and cytotoxicity. J Immunol Methods. 1993; 160: 81-88.
64. Palsson BO. *Systems Biology: Properties of Reconstructed Networks,* New York, Cambridge University Press. 2006; p1-335.
65. Collins S & Bell G. Phenotypic consequences of 1,000 generations of selection at elevated CO2 in a green alga, Nat. 2004; 431: 566-569.
66. Moroney JV & Ynalvez RA, Proposed carbon dioxide concentrating mechanism in *Chlamydomonas reinhardtii*. Eukaryot Cell. 2007; 6: 1251-1259.
67. Rebeille F & Gans P. Interaction between chloroplasts and mitochondria in microalgae - role of glycolysis. Plant Physiology. 1988; 88: 973-975.
68. Kim DH, Ji YH, Jung EA, Han MJ & Kobashi K. Purification and characterization of beta-

glucuronidase from *Escherichia-coli* HGU-3, a human intestinal bacterium. Biol Pharm Bull. 1995; 18: 1184-1188.

69. Eberhard S, Drapier D & Wollman FA. Searching limiting steps in the expression of chloroplast-encoded proteins: relations between gene copy number, transcription, transcript abundance and translation rate in the chloroplast of *Chlamydomonas reinhardtii*. Plant J. 2002; 31: 149-160.
70. Rochaix JD. Post-transcriptional regulation of chloroplast gene expression in *Chlamydomonas reinhardtii*. Plant Mol. Biol 1996; 32: 327-341.
71. Ellis RJ. Most abundant protein in the world. Trends in Biochem Sci. 1979; 4: 241-244.
72. Hsieh S I, Castruita M, Malasarn D, Urzica E, Erde J, Page MD, Yamasaki H, Casero D, Pellegrini M, Merchant SS & Loo JA. The Proteome of Copper, Iron, Zinc, and Manganese Micronutrient Deficiency in *Chlamydomonas reinhardtii*. Mol Cell Proteomics. 2013; 12: 65-86.
73. Maul JE, Lilly JW, Cui LY, Depamphilis CW, Miller W, Harris EH & Stern DB. The Chlamydomonas reinhardtti plastid chromosome: Islands of genes in a sea of repeats. Plant Cell. 2002; 14: 2659-2679.
74. Taylor TC, Backlund A, Bjorhall K, Spreitzer RJ & Andersson I. First crystal structure of rubisco from a green alga, *Chlamydomonas reinhardtii*. J Biol Chem. 2001; 276: 48159-48164.
75. La Fontaine S, Quinn JM, Nakamoto SS, Page MD, Gohre V, Mosely JL, Kropat J & Merchant S. Copper-dependent iron assimilation pathway in the model photosynthetic eukaryote *Chlamydomonas reinhardtii*. Eukaryot Cell. 2002; 1: 736-757.
76. Kirk DL & Kirk MM. Amino-acid and urea uptake in 10 species of *Chlorophyta*. J Phycol. 1978a; 14: 198-203.
77. Kirk DL & Kirk MM. Carrier-mediated uptake of arginine and urea by *Chlamydomonas-reinhardtii*. Plant Physiol. 1978b; 61: 556-560.
78. Reynoso GT & Degamboa BA. Salt tolerance in the fresh-water algae *Chlamydomonas-reinhardii* - effect of proline and taurine. Comp Biochem Physiol a-Physiol. 1982; 73: 95-99.
79. Munozblanco J, Hidalgomartinez J & Cardenas J. Extracellular deamination of L-amino-acids by *Chlamydomonas-reinhardtii* cells. Planta. 1990; 182: 194-198.
80. Zuo Z, Rong Q, Chen K, Yang L, Chen Z, Peng K, Zhu Y, Bai Y & Wang Y. Study of amino acids as nitrogen source in *Chlamydomonas reinhardtii*. Phycol Res. 2012; 60: 161-168.
81. Piedras P, Pineda M, Munoz J & Cardenas J. Purification and characterization of an L-amino-acid oxidase from *Chlamydomonas-reinhardtii*. Planta. 1992; 188: 13-18.
82. Vallon O, Bulte L, Kuras R, Olive J & Wollman FA. Extensive accumulation of an extracellular L-amino-acid oxidase during gametogenesis of *Chlamydomonas-reinhardtii*. Eur J Biochem. 1993; 215: 351-360.

83. Ullrich WR, Larsson M, Larsson CM, Lesch S & Novacky A. Ammonium uptake in lemna-gibba g-1, related membrane-potential changes, and inhibition of anion uptake. Physiol Plant. 1984; 61: 369-376.
84. Byrne TE, Wells MR & Johnson CH. circadian-rhythms of chemotaxis to ammonium and of methylammonium uptake in *Chlamydomonas*. Plant Physiol. 1992; 98: 879-886.
85. Franco AR, Cardenas J & Fernandez E. 2 different carriers transport both ammonium and methylammonium in *Chlamydomonas-reinhardtii*. J Biol Chem. 1998; 263: 14039-14043.